



Failure Modes of Silicon Powder Negative Electrode in Lithium Secondary Batteries

Ji Heon Ryu, Jae Woo Kim, Yung-Eun Sung, and Seung M. Oh^{*,z}

School of Chemical Engineering and Research Center for Energy Conversion and Storage,
Seoul National University, Seoul 151-744, Korea

Si composite negative electrodes for lithium secondary batteries degrade in the dealloying period with an abrupt increase in internal resistance that is caused by a breakdown of conductive network made between Si and carbon particles. This results from a volume contraction of Si particles after expansion in the previous alloying process. Due to the large internal resistance, the dealloying reaction is not completed while Si remains as a lithiated state. The anodic performance is greatly improved either by applying a pressure on the cells or loading a larger amount of conductive carbon in the composite electrodes.
© 2004 The Electrochemical Society. [DOI: 10.1149/1.1792242] All rights reserved.

Manuscript submitted January 7, 2004; revised manuscript received March 10, 2004. Available electronically September 3, 2004.

Si has been emerging as a new negative electrode material for lithium secondary batteries. Even if its theoretical specific capacity is much higher than that of graphite, its commercial use is still hindered.^{1,2} Two major problems are encountered in this material: one is the severe volume change upon charge-discharge cycling and the other is the low electronic conductivity that is inherited from its low bulk conductivity ($6.7 \times 10^{-4} \text{ S cm}^{-1}$) and the presence of oxide layer on Si surface.^{3,4} To solve the first problem, Si negative electrodes were prepared with nano-sized Si powders and a partial improvement was achieved by reducing the absolute volume change.⁵⁻⁷ For the second problem, Si powders were fabricated as a composite with conductive carbon, metal or ceramic materials.⁸⁻¹⁵

The prime concern in this work is the identification of failure modes in Si powder negative electrodes. It is likely that the failure modes are deeply related with severe volume change and poor conductivity. Even if these two features are already known, the details on how these two problematic features play in degrading Si anodes are not fully understood.

Experimental

Si powder (Aldrich Chem. Co., 10 μm average diam) was used as the negative electrode material. Poly(vinylidene fluoride) (PVdF) and Super P were used as the polymeric binder and additive for conductivity enhancement, respectively. To prepare the composite anodes, the mixture of Si powder, Super P and PVdF (8:1:1 in weight ratio) was dispersed in *N*-methyl pyrrolidone (NMP) and homogenized for 2 h. The resulting slurry was spread on a piece of copper foil (25 μm thick and 1 cm^2 apparent area) and dried in vacuum at 120°C for 12 h. The electrode was further roll-pressed to enhance the interparticle contact and to ensure a better adhesion to the current collector.

Half-cell characteristics were analyzed in a beaker-typed three-electrode cell, where lithium foil (Cyprus Co.) was used as the counter and the reference electrode. Pouch-type cells were also fabricated to examine the half-cell characteristics under pressure. To this end, Li foil, porous polypropylene membrane and composite anode film were stacked (1 \times 1 cm) and inserted in a plastic bag named as Poly bags (Aldrich Chem. Co.). The used electrolyte was 1.0 M LiClO_4 in ethylene carbonate (EC)/diethyl carbonate (DEC) (1:1 volume ratio) (Tomiya Co.). Galvanostatic charge-discharge cycling was made with a gravimetric current density of 100 mA g^{-1} and voltage cutoff range of 0.0-2.0 V (vs. Li/Li^+). The galvanostatic intermittent titration technique (GITT) was employed to monitor the evolution of internal resistance during cycling, where a current pulse of 100 mA g^{-1} was applied for 10 min to measure the closed-circuit voltage (CCV) and turned off for 20 min to obtain the quasi-open-circuit voltage (QOCV). The sequential current pulse was applied

for both charging and discharging period in the range of 0.0-2.0 V. Internal resistance was calculated from the difference between the CCV and QOCV in each voltage transient. All electrochemical measurements were made with a WBCS-3000 battery cycler (Xeno Co.) at ambient temperature in a glove box filled with argon.

Results and Discussion

Figure 1 shows the galvanostatic charge-discharge voltage profiles obtained with a Si power anode, where several features are immediately apparent. First, there appears a large amount of irreversible capacity in the first cycle. The first charging capacity amounts to 3260 mAh g^{-1} but the electrode discharges only 1170 mAh g^{-1} . Strangely, the irreversible capacity related to the solid electrolyte interface (SEI) formation is negligible. This is somewhat unusual considering the graphite anodes that always exhibit a voltage plateau near 0.8-1.0 V as a result of SEI formation. The absence of SEI formation in Si anodes has been reported in the previous literature,¹⁶ where it was claimed that electrolyte decomposition is greatly reduced due to the oxide layer on Si surface. Second, the irreversible capacity loss is observed in every cycle. For instance, in the third cycle, the charging and discharging capacity is 780 and 630 mAh g^{-1} , respectively. This feature is also contrasting with the graphite anodes, where the irreversible capacity loss is encountered only within the initial 1-2 cycles. Third, the charging capacity in each cycle is comparable to the discharging capacity in the previous cycle. For instance, the second charging capacity (1100 mAh g^{-1}) is close to the first discharging capacity (1170 mAh g^{-1}) and the third charging capacity to the second discharging, indicating that almost of the empty Li^+ storage sites generated in the previous dealloying reaction are utilized for the next alloying reaction. This observation strongly suggests that the Si composite electrodes degrade in the dealloying period rather than in the charging. Finally, Li^+ ions are successively accumulated inside the Si matrix as an alloy state due to the feature characterized by a rather complete charging but incomplete discharging in each cycle.

The galvanostatic intermittent titration technique was used to examine the causes for incomplete discharging and Li^+ trapping in the Si matrix. Figure 2a presents the overall transient voltage profile obtained in the first cycle. A typical voltage transient observed in one current pulse cycle is represented in the inset, where it is seen that a fast voltage drop is observed in the initial period due to the ohmic resistance but rather slow decay in the later stage due to the charge transfer resistance. Upon current pulse being turned off, however, voltage restores to the initial quasi-equilibrium value. The uppermost trace in the charging profile in Fig. 2a thus corresponds to the QOCV while the bottom one the CCV. In contrast, the uppermost trace in the discharging period represents the CCV. The internal resistance was calculated from the difference between QOCV and CCV in each voltage transient and displayed in Fig. 2b. One apparent feature in Fig. 2b is that the internal resistance of Si composite anode steadily decreases in the charging period, but rather

* Electrochemical Society Active Member.

^z E-mail: seungoh@plaza.snu.ac.kr

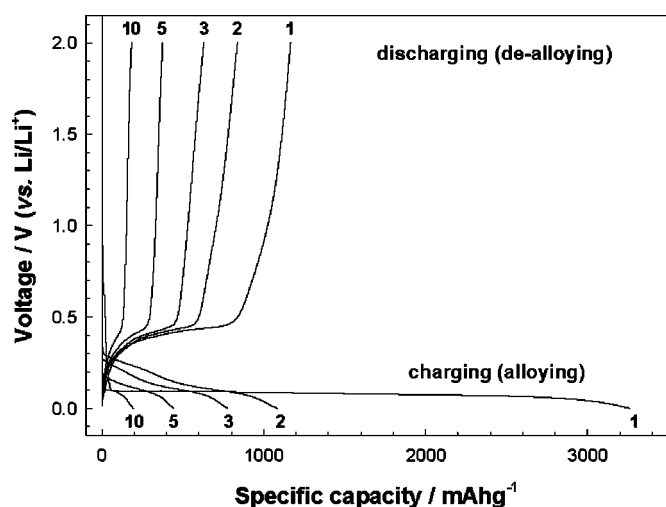


Figure 1. Galvanostatic charge-discharge voltage profiles obtained with a silicon powder anode. The composite anode was made with silicon powder (10 μm average diam), Super P (conducting agent) and PVdF (binder) (8:1:1 in weight ratio). The gravimetric current density was 100 mA g^{-1} and the voltage cut-off range was 0.0-2.0 V (vs. Li/Li^+).

rapidly below 0.3 V. In the discharging period, however, a sudden increase in internal resistance is observed from 0.4 V. Note that a similar change was evolved in the next cycles.

The variation of internal resistance envisions what happens in the Si composite anode during cycling. In Si composite anode, the Si powder and carbon particles are dispersed to have large contact area between two components. Upon charging, Si reacts with Li^+ ions and electrons with a volume expansion, which allows a better contact between Si and carbon particles inside the composite anode. The noticeable drop in internal resistance below 0.3 V can thus be explained by the fact that the alloying reaction takes place mainly below 0.3 V as seen in the charging profiles in Fig. 1. That is, the volume expansion should be most significant below 0.3 V. A slightly higher electrical conductivity of lithiated Si (Li_xSi) than that of pure Si may be another explanation for the resistance drop.¹⁷ Upon dealloying, however, Si particles contract, causing poor contact with carbon and eventually the isolation of the particles from the electronic path made between current collector to carbon particles as the whole electrode layer is not elastic enough. The loss of electronic path brings about an increase in both the contact (ohmic) resistance and charge transfer resistance for dealloying reaction. Eventually, due to the huge internal resistance, the electrode potential reaches earlier at the discharging cutoff limit (2.0 V) while the dealloying reaction being incomplete. The volume contraction is most serious above 0.4 V because the dealloying reaction takes place mainly in this voltage range, which explains the abrupt resistance increase above 0.4 V. This peculiar feature must be resulted from the enormous volume change and low electronic conductivity of lithiated Si. If the lithiated Si is conductive enough like graphite materials, the dealloying reaction may take place over the whole surface of Si particles even in this undesirable situation since electrons generated from the dealloying reaction can be transferred to current collector through the conductive Si surface and carbon particles. Because this is not the case, however, the dealloying reaction is possible only at the intimate contact points made with carbon particles. In the forthcoming charging period, Si particles expand again to gain a better contact with carbon such that the alloying reaction is continued without a severe polarization until the electrode potential reaches at the charging limit (0.0 V). The next charging capacity is, however, limited only up to the discharging capacity in the previous cycle because the available sites for alloying reaction are those generated in the previous dealloying process.

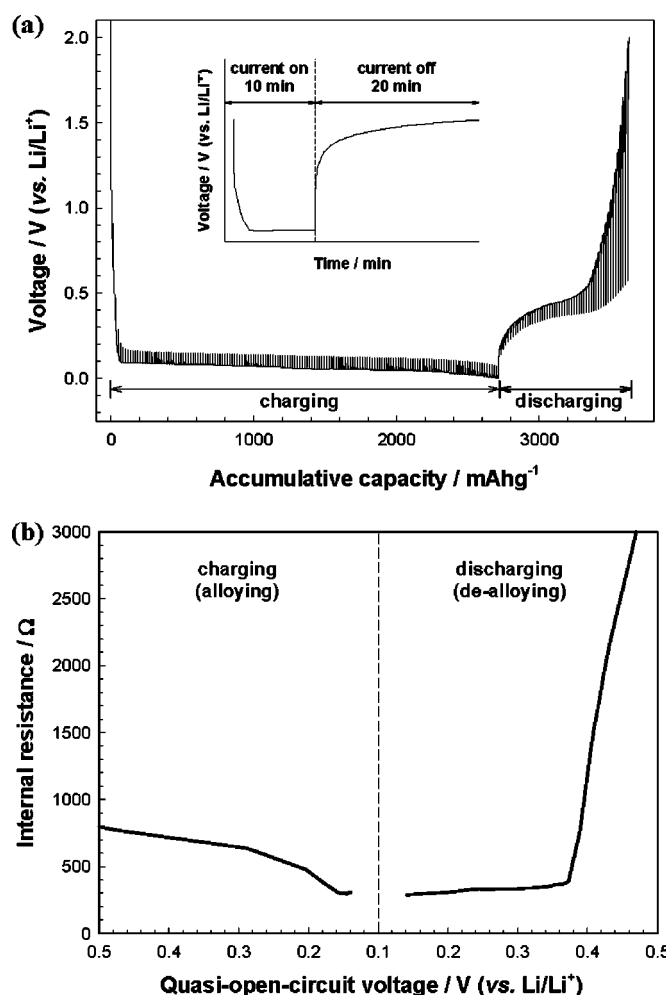


Figure 2. (a) Transient voltage profiles obtained with GITT. Inset: A typical voltage transient traced in one current pulse cycle. (b) The evolution of internal resistance in Si composite anode calculated from the transient voltage profiles.

To ascertain the incomplete discharging and accumulation of Li^+ inside the Si matrix, a control experiment was made with pouch-type cells, with which pressure imposition was possible. For this experiment, the galvanostatic cycling was stopped after the third discharging. At this moment, the composite anode is supposed to be highly lithiated due to the successive Li^+ accumulation. After the current being turned off, the OCV of anode steadily decreased to reach at 0.33 V after 12 h (Fig. 3a). When discharged at this stage under the galvanostatic condition, the delivered capacity was negligible. When a pressure was applied, however, the OCV decreased from 0.33 to 0.27 V in proportional to the applied pressure, as indicated in Fig. 3a. More interestingly, when this electrode was discharged under pressure, additional capacity up to 712 mAh g^{-1} was observed (Fig. 3b).

The result of the pressure experiment supports the proposed failure mechanism. It is seemingly after the third discharging that the Si particles carry a widely different degree of lithiation as the composite anode layer is swollen with a poorly conducting network, some of which are electronically connected via carbon particles to the current collector while others are isolated. The discharge capacity (370 mAh g^{-1}) obtained in the third cycle must be delivered by the Si particles that are electronically connected to the current collector. Also, the degree of lithiation in these Si particles is somewhat lower than that of the isolated ones. The negligible discharging after 12 h duration at the open-circuit condition illustrates that the conducting

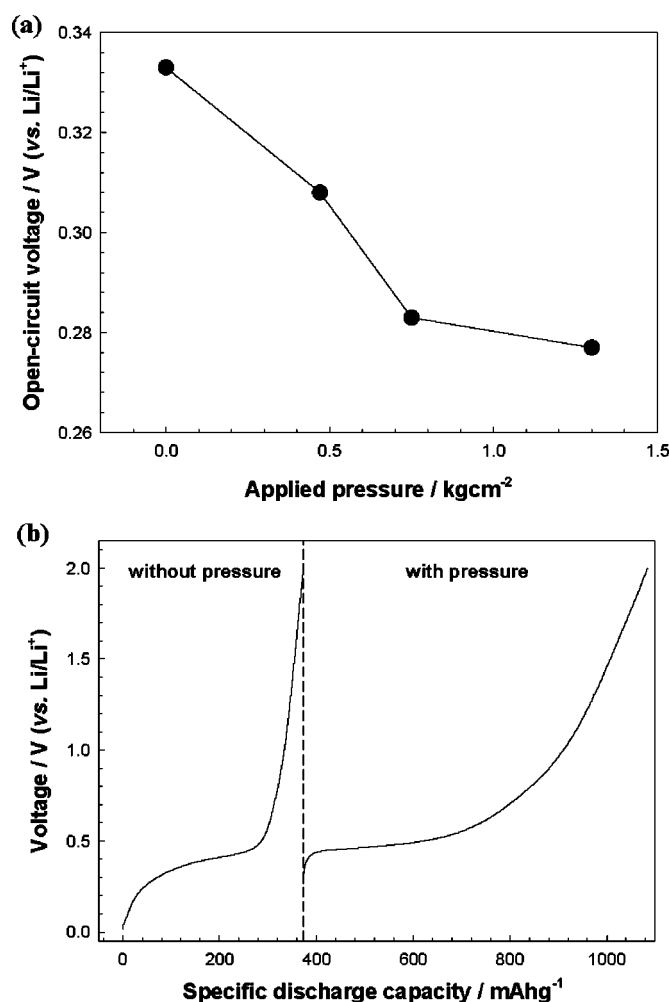


Figure 3. (a) OCV against the applied pressure observed with a pouch-type cell. (b) The galvanostatic discharge voltage profile recorded under the normal discharging condition (left side) and that obtained under a pressure imposition (1.3 kg cm^{-2}) (right side). The electrode composition was the same as for Fig. 1.

network is not restored in normal condition, which further manifests itself that the electrode layer is not elastic. Upon a pressure imposition, however, the lithiated Si particles having a lower degree of lithiation are now connected to the highly lithiated or even isolated ones either by a direct contact or via carbon particles, under which condition Li⁺ ions are redistributed among the Si particles. Now, a larger fraction of Si particles are connected to the current collector and their degree of lithiation is higher than before. This can account for the decrease in the rest potential upon a pressure imposition because a lower rest potential reflects a higher degree of lithiation. Also, as the conduction network is rebuilt, additional dealloying reaction is possible upon discharging.

In summary, the larger contact area between Si and carbon particles seems to be one of the requirements, among others, to achieve a better cyclability. To confirm this, Si composite electrodes were fabricated with a different carbon loading and their cyclability was compared to each other. As demonstrated in Fig. 4, the first discharge capacity and cyclability is greatly improved with a higher carbon loading. Also, an improvement is observed with a pressure imposition.

As a summary, the poor cyclability of Si powder anode originates from two problematic features involved in Si powder; a large volume change and poor electronic conductivity. To overcome these problems, two solutions may be proposed. One is the use of elasto-

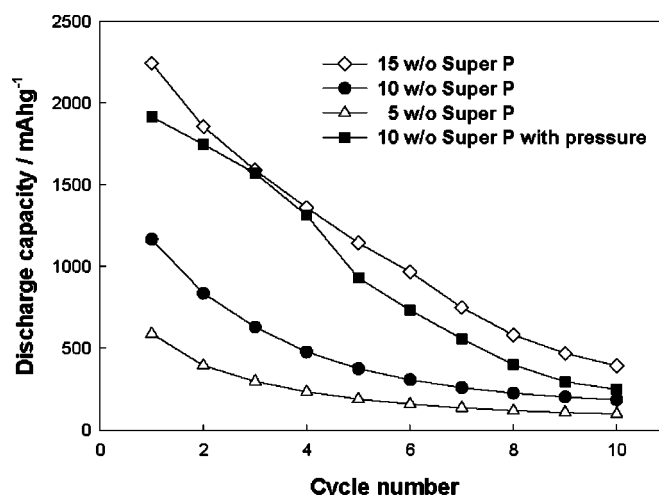


Figure 4. Specific discharge capacity (based on Si weight) measured with a variation in carbon loading. The binder content was the same as for the carbon. The result obtained under a pressure of 1.3 kg cm^{-2} is also presented for comparison.

meric polymer binder as it is expected that the contact area between Si and carbon particles is restored even after a repeated volume change. The use of Si composite materials or surface-coated Si with highly conductive carbon, ceramic and metal may be the other solution.

Conclusions

The failure modes in Si powder anodes have been identified and the possible solutions provided. The following points are summarized.

The major capacity fading occurs in the discharging period rather than in the charging period. In the discharging process, the dealloying reaction is not completed due to an abrupt increase in internal resistance that is caused by a loss of contact area between Si and carbon particles. This unfavorable feature is in turn caused by a volume contraction of Si particles after expansion in the previous alloying period. Due to the limited contact between two components and also due to the poor conductivity of lithiated Si, the dealloying reaction takes place only at or nearby the contact area.

Si anodes are degraded as a lithiated state because the dealloying reaction is not completed in each cycle. Upon a pressure imposition at this stage, additional dealloying reaction is possible as the conducting network is rebuilt. A pressure imposition or loading a larger amount of carbon allows a better performance by ensuring a better contact between two components. As a countermeasure, the use of elastomeric polymer binder, and the composites or surface coating with conductive materials is proposed.

Acknowledgment

This work was partially supported by KOSEF through Research Center for Energy Conversion and Storage, and by the financial support of "Center for Nanostructured Materials Technology" under "21st Century Frontier R&D Programs" of the Ministry of Science and Technology, Korea. Financial support from LG Chem. Ltd. is also acknowledged.

Seoul National University assisted in meeting the publication costs of this article.

References

1. C. J. Wen and R. A. Huggins, *J. Solid State Chem.*, **37**, 271 (1981).
2. J. O. Besenhard, J. Yang, and M. Winter, *J. Power Sources*, **68**, 87 (1997).
3. L. Y. Beaulieu, K. W. Eberman, R. L. Turner, L. J. Krause, and J. R. Dahn, *Electrochem. Solid-State Lett.*, **4**, A137 (2001).
4. M. Yoshio, H. Wang, K. Fukuda, T. Umeno, N. Dimov, and Z. Ogumi, *J. Electrochem. Soc.*, **149**, A1598 (2002).

5. A. M. Wilson and J. R. Dahn, *J. Electrochem. Soc.*, **142**, 326 (1995).
6. H. Li, X. Huang, L. Chen, Z. Wu, and Y. Liang, *Electrochem. Solid-State Lett.*, **2**, 547 (1999).
7. H. Li, X. Huang, L. Chen, G. Zhou, Z. Zhang, D. Yu, Y. J. Mo, and N. Pei, *Solid State Ionics*, **135**, 181 (2000).
8. H. Y. Lee and S. M. Lee, *J. Power Sources*, **112**, 649 (2002).
9. W. J. Weydanz, M. Wohlfahrt-Mehrens, and R. A. Huggins, *J. Power Sources*, **81-82**, 237 (1999).
10. S. M. Hwang, H. Y. Lee, S. W. Jang, S. M. Lee, S. J. Lee, H. K. Baik, and J. Y. Lee, *Electrochem. Solid-State Lett.*, **4**, A97 (2001).
11. I. S. Kim, G. E. Blomgren, and P. N. Kumata, *Electrochem. Solid-State Lett.*, **6**, A157 (2003).
12. N. Dimov, S. Kugino, and M. Yoshio, *Electrochim. Acta*, **48**, 1579 (2003).
13. J. Yang, B. F. Wang, K. Wang, Y. Liu, J. Y. Xie, and Z. S. Wen, *Electrochem. Solid-State Lett.*, **6**, A154 (2003).
14. Z. S. Wen, J. Yang, B. F. Wang, K. Wang, and Y. Liu, *Electrochem. Commun.*, **5**, 165 (2003).
15. L. Y. Beaulieu, K. C. Hewitt, R. L. Turner, A. Bonakdarpour, A. A. Abdo, L. Christensen, K. W. Eberman, L. J. Krause, and J. R. Dahn, *J. Electrochem. Soc.*, **150**, A149 (2003).
16. X. D. Wu, Z. X. Wang, L. Q. Chen, and X. J. Huang, *Electrochem. Commun.*, **5**, 935 (2003).
17. L. A. Stearns, J. Gryko, J. Diefenbacher, G. K. Ramachandran, and P. F. McMillan, *J. Solid State Chem.*, **173**, 251 (2003).